Dev Genes Evol (2010) 220:139–149
DOI 10.1007/s00427-010-0335-3

ORIGINAL ARTICLE

The proliferation and migration of immature germ cells in the mussel, *Mytilus galloprovincialis*: observation of the expression pattern in the *M. galloprovincialis vasa*-like gene (*Myvlg*) by in situ hybridization

Mayu Obata · Natsumi Sano · Shunsuke Kimata · Kazue Nagasawa · Goro Yoshizaki · Akira Komaru

Received: 22 January 2010 / Accepted: 24 July 2010 / Published online: 20 August 2010

Abstract In bivalve, the distribution of primordial germ cells can be traced from early embryogenesis to the veliger larva by the expression of the *vasa* ortholog. However, the distribution of germ cells from metamorphosis to maturation in bivalves has not been examined extensively. In this study, we used in situ hybridization to observe expression of the *Mytilus galloprovincialis vasa*-like gene (*Myvlg*). The distribution of germ cells was clarified in immature mussels. We observed germ cells in adult mussels during the non-reproductive and reproductive seasons. *Myvlg* was specifically expressed in germ cells. Gametogenesis occurs in acini surrounded by connective tissue. *Myvlg* expression was detected in spermatogonia, spermatocytes, oogonia, and oocytes. In the non-reproductive season, gametes were not observed in the acini, but *Myvlg* was expressed in germinal stem cells along the acini. The expression intensity in the non-reproductive season, however, was much weaker than that in the reproductive season. *Myvlg*-positive cells proliferated during the non-reproductive season. In immature mussels, a pair of germ cell clumps was distributed laterally in the connective tissue between the nephric tubules and posterior byssal retractor muscle. Germ cells were also observed along pericardium. When immature mussels grew, a pair of germ cell clumps migrated anteriorly in the connective tissue along the outer epithelium at the dorsal region of the mantle base between the mantle and gill. The number of germ cells increased significantly as the mussels grew. This is the first report to observe the proliferation and migration of germ cells in immature mussels.

Keywords *Vasa* · Germ cell · *Mytilus galloprovincialis* · In situ hybridization

Communicated by D.A. Weisblat

M. Obata (✉) · N. Sano · S. Kimata · A. Komaru
Faculty of Bioresources, Mie University,
1577 Kurimamachiya,
Tsu, Mie 514-8507, Japan
e-mail: mayu_obata@bivalve.sakura.ne.jp

K. Nagasawa · G. Yoshizaki
Department of Marine Biosciences,
Tokyo University of Marine Science and Technology,
4-5-7 Konan,
Minato-ku, Tokyo 108-8477, Japan

Introduction

The origin of germ line cells has been studied for over a 100 years. In many animal species, the germ cell contains a structural feature called a nuage (Eddy 1975). The nuage is an electron-dense cytoplasm containing mitochondria, RNA, and protein. It is widely believed to carry the determinants of the germ line (Saffman and Lasko 1999). Thus, the distribution of primordial germ cells (PGCs) has been studied by observation of nuages in many animal species (Woods 1932; Heasman et al. 1984).

Recently, *vasa* orthologs have been used as a specific germ line molecular marker in many animal species. *Vasa* was first identified in *Drosophila* as a maternally supplied factor required for posterior patterning and germ line cell development (Hay et al. 1988). VASA encodes a protein member of the DEAD-box family. It is suggested that *vasa* acts as a translational regulator in the oocytes (Saffman and Lasko 1999). The expression pattern is restricted to the germ line cells. A *vasa* ortholog has been isolated and used as a molecular marker to detect PGCs and other germ line

cells from many animals (Roussel and Bennett 1993; Fujiwara et al. 1994; Komiya et al. 1994; Olsen et al. 1997; Castrillon et al. 2000; Mochizuki et al. 2001; Fabioux et al. 2004).

In bivalve species, gonads consist of gonadal acini connected with the genital canal. The location of the gonads varies among bivalve species. For example, in Pectinidae, gonads are observed as distinct organs, as in vertebrates and insects. In other bivalve species, such as Mytilidae and Anomiidae, gonads are formed in the connective tissue, both in the visceral mass and mantle. Thus, the gonads of most bivalve species are apparently observed in the connective tissue rather than as a distinct organ.

In bivalve species, studies on the formation of germ line cells are limited. The distribution of bivalve PGCs was examined in *Sphaerium striatinum* embryos by observing, under the light microscope, the presence of mitochondria-dense cytoplasm-like nuages in early development (Woods 1932). Woods (1932) reported that PGCs were derived from 4d cells. In bivalves and gastropods, the *vasa* ortholog has been used recently as a germ line-specific marker. The distribution of PGCs was observed by in situ hybridization (ISH) of the *vasa* ortholog in an oyster and mud snail (Fabioux et al. 2004; Swartz et al. 2008). Fabioux et al. (2004) revealed that PGCs are derived from Mr and M1 cells arising from the mesodermal 4d blastomere, confirming the observation of Woods (1932). They observed the distribution of PGCs as far as the veliger larval stage. Veliger larvae metamorphose into mussels after 1 month. However, there are few reports that have traced the distribution of immature germ cells from metamorphosis to maturation in bivalves (Woods 1931).

The reproductive cycles of many bivalve species have been studied, including the mussel, *Mytilus galloprovincialis* (Mytilidae) (Kautsky 1982; Newell et al. 1982). In this species, the mantle and each organ in the visceral mass is supported by connective tissue. Connective tissue consists of two cell types; adipo-granular (ADG) and visceral connective tissue (VCT) (Pipe 1987). During the reproductive season, gonadal acini are produced between ADG and VCT (Lubet 1959; Lowe et al. 1982). At the end of the reproductive season, however, the germ cells of the connective tissue degenerate in the mantle and visceral mass (Pipe 1987). Remaining gametes are resorbed by the epithelial cells of the gonoduct. In bivalves, however, the position of the germ line cells during the non-reproductive season has not been studied extensively (Lubet 1959, Fabioux et al. 2004).

The purpose of this study was to determine the distribution of the germ cells during the reproductive cycle of *M. galloprovincialis*. We isolated a *M. galloprovincialis vasa*-like gene (*Myvlg*) as a specific germ line molecular marker. The distribution and proliferation of immature germ cells were examined from metamorphosis to maturation. We observed the *Myvlg* expression pattern in immature mussels, adult mussels during the non-reproductive season, and mature mussels in the reproductive season with in situ hybridization.

Materials and methods

Sampling

M. galloprovincialis were collected from the intertidal zone at Akogi, in the city of Tsu, Mie Prefecture, Japan. For RNA extraction, mussels were collected from November to February 2007. For in situ hybridization, immature mussels (shell height ranged from 2 to 15 mm) were collected from May to August 2008, and mature mussels (shell height ranged from 30 to 50 mm) were collected from November to February 2007. Adult mussels (shell height ranged from 50 to 80 mm) were also collected during the non-reproductive season, from July to September 2007 and 2009.

RNA extraction and cDNA cloning

Small pieces of ovary and testis were frozen at −80°C for RNA extraction. Total RNA was isolated from the ovary and testis using a TRIzol Plus RNA Purification kit (Invitrogen, Carlsbad, CA, USA). cDNA was synthesized with Ready-To-Go™ You-Prime First-Strand Beads (GE Healthcare, Buckinghamshire, UK) and Oligo dT primers (R&D SYSTEMS, Minneapolis, MN, USA), according to the manufacturer's protocol. Degenerate primers were designated to amplify the *M. galloprovincialis vasa*-like gene: Forward (5′-ATGGCNTGYGCNCARACNGG-3′) and Reverse (5′-RAANCCCAT RTCYAACAT-3′). Degenerate polymerase chain reaction (PCR) was performed with the following cycles: 94°C for 30 s, 52°C for 30 s, 72°C for 60 s (total of 30 cycles). Approximately 400-bp fragments were amplified from each cDNA. These PCR products were purified by agarose gel electrophoresis, cloned into pGEM®-T Easy Vector (Promega, Madison, WI, USA) and sequenced with a 3100 Genetic Analyzer automatic sequencer (ABI, Foster City, CA, USA) using DYEnamic™ ET terminator kit Cycle Sequencing Kit (GE Healthcare).

5′- and 3′-RACE of *vasa*-like cDNA

Rapid amplification of 5′ cDNA ends (5′ RACE) was carried out with a 5′-Full RACE Core Set (TaKaRa) according to the manufacturer's instructions using 5′-end phosphorylated

gene-specific primer RTP1 (5′-(p)CTACCAGGTGTACCA) and two pairs of primers: 5-1F (5′-GGAGGA ACCTCTCTTGGACA) and 5-1R (5′-AAG CCTGTGGCTCCTGAAC), 5-2F (5′-ACTGAGGAATGT AGAACAGGG), and 5-2R (5′-CCGGTCTGCGCACA CGCCAT). Rapid amplification of 3′ cDNA ends (3′ RACE) was carried out with a 3′-Full RACE Core Set (TaKaRa) according to the manufacturer's instructions using the gene-specific primer GSP1 (5′-GTTCAGGAGCCACAGGCTT). The PCR product was cloned and the sequence determined. Amino acids were determined by cDNA sequence, and protein domains were predicted by the modular architecture research tool, SMART (Schultz et al. 1998).

Phylogenetic analysis of DEAD box family protein

Phylogenetic analysis was realized with a range of DEAD-box proteins belonging to the VASA, PL10, and p68 subfamilies, from vertebrates and invertebrates. The amino acid sequences were aligned using Clustal W. The genetic relationships between the *M. galloprovincialis* VASA-related protein and VASA-related proteins of other species were estimated in Mega 4.0.2 (Tamura et al. 2007) using the neighbor-joining (Saitou and Nei 1987) method of clustering based on a PAM Matrix (Dayhoff et al. 1978). Bootstrap values were computed over 1,000 replications.

Section preparation

The mussels were fixed with aqueous Bouin's fluid for in situ hybridization. After fixation, the shell of the immature mussels was removed with tweezers. Fixed samples were dehydrated in an ethanol series and embedded in paraffin wax. Six-micrometer sections were cut, mounted, and stained with a *Myvlg*-specific probe. Whole bodies of mature mussels were sectioned and stained with hematoxylin and eosin (HE) to observe the location of the gonad.

In situ hybridization

About 950 bp sequences of *Myvlg* were used as probes for in situ hybridization, prepared using a DIG RNA labeling kit with T7 RNA polymerase (Roche, Indianapolis, IN, USA), and used at a concentration of 1 μg/ml in the hybridization buffer. In situ hybridization was performed according to the method described by Wilkinson and Nieto (1993) with the following modification. Proteinase K treatment (1 μg/ml) was carried out for 15 min at 37°C. Hybridization was performed at 65°C overnight. Blocking was performed with Blocking Reagent (Roche) before the antibody reaction. A mixture of BCIP/NBT was used for color development of the anti-Digoxigenin-AP Fab fragments (Roche). After in situ hybridization, each sample was counterstained by Nuclear Fast red (VECTOR, Burlingame, CA, USA) or eosin and observed under a Nikon E600 (Nikon, Tokyo, Japan) light microscope.

The number of *Myvlg*-positive cells was counted in the mantle of mussels from the non-reproductive season and from just before the reproductive season. A part of mantle was cut and observed. *Myvlg*-positive cells were counted in two 5×5 mm areas selected at random from each individual. The number of *Myvlg*-positive cells was also counted in immature mussels. Whole immature mussels were cut from posterior to anterior and serial sections were prepared. All sections were observed, and the number of germ cells was counted in each section.

Results

Isolation of the *M. galloprovincialis vasa*-like gene cDNA

A single fragment of approximately 400 bp was amplified from female and male gonads by degenerate PCR. The 5′ and 3′ ends of this sequence were obtained by RACE-PCR. The total isolated sequence was 3,478 bp. This sequence comprised a 5′ untranslated region of 81 bp, an open reading frame of 2,235 bp and a 3′ untranslated region of 1,162 bp. The amino acid sequence was 745aa long (Fig. 1a). This included two RGG (arginine-glycine-glycine) motifs, four Zn-fingers, glycine-rich regions, a c-terminal DEAD-box motif, and a helicase superfamily c-terminal domain (Fig. 1a, b), which are characteristic of VASA-like proteins. Analysis of the phylogenetic relationship in the DEAD-box protein family showed that the isolated amino acids are included in the VASA sub-family, and not the PL10 sub-family (Fig. 2).

Observation of the gonad of adult mussels during the reproductive season

Cross-sections of the whole body were cut at the center of the foot (Fig. 3a), and stained with HE. The visceral mass and mantle were supported with connective tissue (Fig. 3b). The gonad could be observed within the connective tissue. Gametogenesis occurs in the acini surrounded by connective tissue. Thus the connective tissue intermediated between the gonad and each organ such as a midgut gland (Fig. 3c). The gonad was also found in the connective tissue between the outer and inner epithelium of the mantle (Fig. 3d).

Germ cell-specific expression of *Myvlg* in the reproductive season by in situ hybridization

We observed gametogenesis in the mantle of adult mussels. In the mature male gonad, spermatogonia, spermatocytes, spermatids and sperm were located in series from the wall

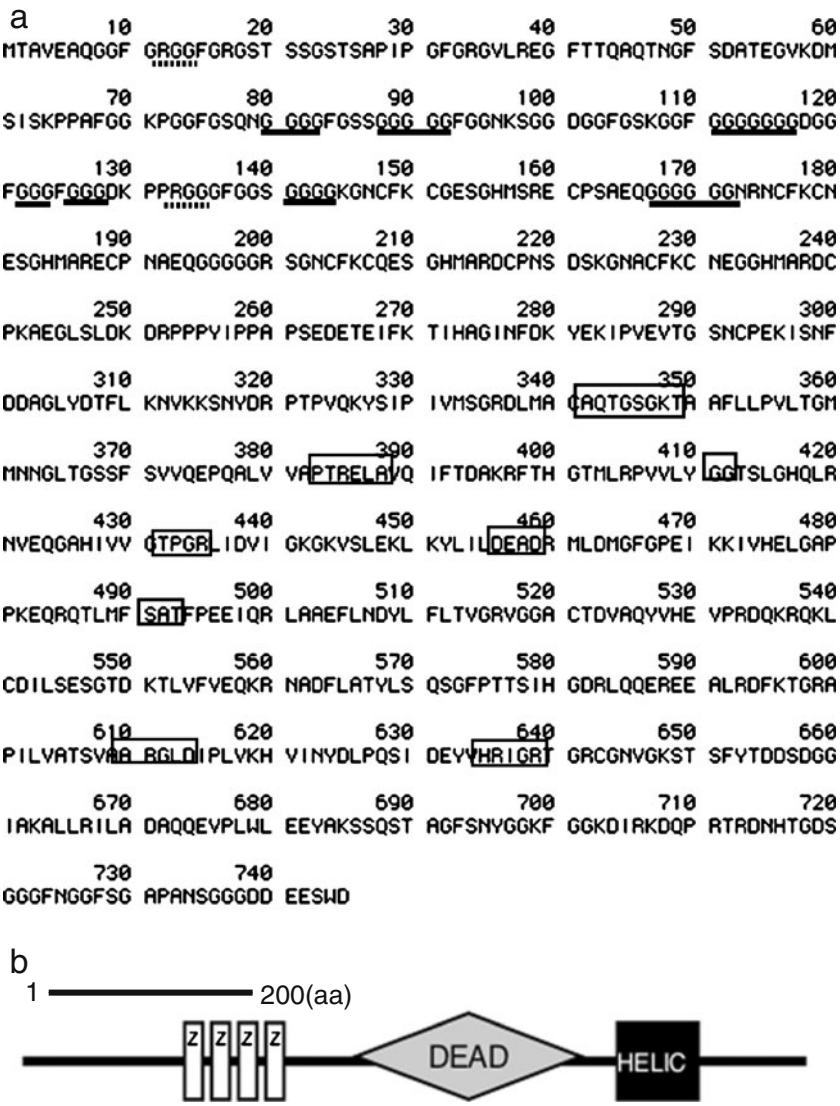

Fig 1 Amino acid sequences and protein domains of the isolated *M. galloprovincialis vasa*-like gene (*Myvlg*). **a** *Myvlg* amino acid sequences. *Black-dotted line* RGG motif, *black line* glycine-rich region, *black box* eight conserved regions of the DEAD-box protein family, **b** protein domains of *Myvlg* amino acids predicted by SMART. *Black bar* shows the length of 200 amino acids. *Z* zinc finger motif, *DEAD* DEAD-like helicases superfamily, *HELIC* helicase superfamily c-terminal domain

of the acinus to its center (Fig. 4a). Spermatogonia that were attached to the wall of the acinus were larger than the spermatocytes. Spermatids and spermatozoa (which had condensed nuclei) were smaller than spermatocytes. *Myvlg* expression was restricted to spermatogonia and spermatocytes (Fig. 4b, c). Spermatogonia stained stronger than spermatocytes (Fig. 4c). The *Myvlg* signal was not detected in spermatids and sperm. In male gonadal sections stained with the sense probe, there was no *Myvlg* signal (Fig. 4d). In the female gonad, flattened oogonia were gathered adjacent to each other along the acinus wall (Fig. 4e). Early oocytes that possessed an obvious nucleus and nucleolus were also located along the acinus wall. Mature oocytes, larger than oogonia and oocytes, were partly attached to the acinus wall. A *Myvlg* signal was stronger in oogonia and early oocytes in comparison with mature oocytes (Fig. 4f, g). In the female gonad stained with the sense probe, there was no *Myvlg* signal (Fig. 4h).

Presence of germ cells and *Myvlg* expression in the adult mussel in the non-reproductive season

In July and August (non-reproductive season), gametes were absent (Fig. 5a) and therefore the sex of mussels could not be determined. The acini had decreased in number and size. The ADG and VCT were well developed around the mantle and visceral mass. Along the base of the acini, some germ cells that were ovoid in shape were observed. The *Myvlg* signal was restricted to the cytoplasm, and its intensity was very weak (Fig. 5b). The size of the long and short axes of the germ cells was 8.1±2.3 μm and 5.3±1.4 μm, respectively. They possessed a large nucleus (5.9±1.3 μm×4.7±1.2 μm) surrounded by a small amount of cytoplasm (Fig. 5b, c).

In September and October, just before the reproductive season, ADG and VCT were still well developed (Fig. 5d). In three of four mussels, the onset of gametogenesis was observed by the presence of developing oocytes. In the

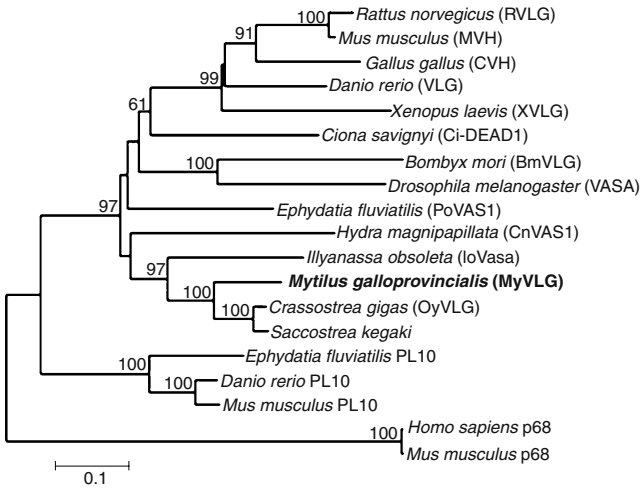

Fig 2 Phylogenetic tree of VASA-related proteins by the neighbor-joining method. The sequences were aligned using Clustal W. Number at each node represents the percentage values given by bootstrap analysis. GenBank accession numbers in each sequence are indicated below. RVHG *Rattus norvegicus* (S75275), MVH *Mus musculus* (BAA03584), CVH *Gallus gallus* (BAB12337), VLG *Danio rerio* (CAA72735), XVLG *Xenopus laevis* (AAC03114), Ci-DEAD1 *Ciona savignyi* (BAA36711), BmVLG *Bombyx mori* (BAA19572), VASA *Drosophila melanogaster* (P09052), PoVAS1 *Ephydatia fluviatilis* (BAB13310), CnVAS1 *Hydra magnipapillata* (BAB13307), IoVasa *Ilyanassa obsoleta* (EU047801), MyVLG *Mytilus galloprovincialis* (AB563493), OyVLG *Crassostrea gigas* (AY423380), *Saccostrea kegaki* (AB374933), *E. fluviatilis* PL10 (BAB13309), *D. rerio* PL10 (NP571016), *M. musculus* PL10 (AAA39942), *Homo sapiens* p68 (P17844), *M. musculus* p68 (CAA46581)

three mussels with oocytes, the long axis of *Myvlg*-positive cells was 15.6±11.6 μm and the short one was 9.0±6.9 μm (Fig. 5d–f). In one mussel without oocytes, the long axis of *Myvlg*-positive cells was 7.6±1.7 μm and the short one was 4.7±1.2 μm. The number of *Myvlg*-positive cells was significantly greater when compared with that of the mussels during the non-reproductive season ($P<0.05$, Mann–Whitney *U* test). The signal intensity was also much stronger than that recorded in the non-reproductive season.

Distribution of germ cells in immature mussels

Immature mussel, (2–5 mm shell height)

At first, the *Myvlg* expression pattern was observed in small immature mussels with a shell height ranging from 2 to 5 mm. The immature mussels were sectioned from posterior to anterior (Fig. 6a). The immature germ cells were supported by connective tissue and distributed laterally between the nephric tubules and posterior byssal retractor muscle (Fig. 6b, c). Germ cells were also observed along the pericardium (Fig. 6d, e). Multiple germ cells formed a cluster, which was attached to flat somatic cells in the acinus at the pericardium (Fig. 6e). The immature germ cells, which measured 6.2±1.0 μm×5.0±1.0 μm, each possessed a large nucleus surrounded by a small amount of cytoplasm (Fig. 6c, e). The germ cells were observed only in the section that included the nephric tubules. The number of germ cells in a mussel was 55.3±28.9 ($n=6$).

Immature mussels (5–15 mm shell height)

Immature mussels ranging from 5 to 15 mm were also sectioned and observed from posterior to anterior (Fig. 7a). In the sections containing nephric tubules, immature germ cells were distributed in the connective tissue at visceral mass (Fig. 7b, c). The germ cells also extended into the dorsal mantle base between the mantle and gills (Fig. 7b, arrows). In the sections that included the foot, immature germ cells were present in the dorsal mantle base between the mantle and gill (Fig. 7d). Multiple immature germ cells gathered, formed a few clusters attached to flat somatic cells in the acinus and apparently migrated along the outer epithelium (Fig. 7e). Immature germ cells migrated along the dorsal mantle base until the anterior byssal retractor muscle appeared near the foot (Fig. 7f, g). In the section with the labial palps, immature germ cells were not observed (Fig. 7h). The number of germ cells was 276.2±139.8 ($n=5$), which is significantly greater than that recorded in the small immature mussels ($P<0.01$, Mann–Whitney *U* test).

Discussion

The *M. galloprovincialis vasa* ortholog

We confirmed that *Myvlg* belongs to the DEAD-box family of proteins like other VASA-like proteins. All DEAD-box proteins are putative ATP-dependent RNA helicases (Hay et al. 1988). *Myvlg* included two ATPase motifs (AQTGSGKT, DEAD), three ATP binding and cleavage motifs (PTRELA, GG, TPGR), two RNA unwinding motifs (SAT, HRIGR), and the helicase C domain (ARGLD). These eight motifs are characteristic of the DEAD-box proteins (Schmid and Linder 1992; Rebscher et al. 2007). The VASA-like proteins have glycine-rich amino acids, zinc finger motifs and a RGG motif at the N-terminal (Shibata et al. 1999; Yoshizaki et al. 2000; Fabioux et al. 2004). *Myvlg* also had multiple glycine-rich regions, two RGG motifs and four zinc finger motifs. Thus, *Myvlg* included characteristic motifs of both the DEAD-box family and VASA-like proteins.

Phylogenetic analysis also revealed that *Myvlg* most closely resembles VASA-like proteins rather than other members of the DEAD-box protein family such as PL10 and p68 sub-family members. In addition, phylogenetic analysis indicated that *Myvlg* is closely related to inverte-

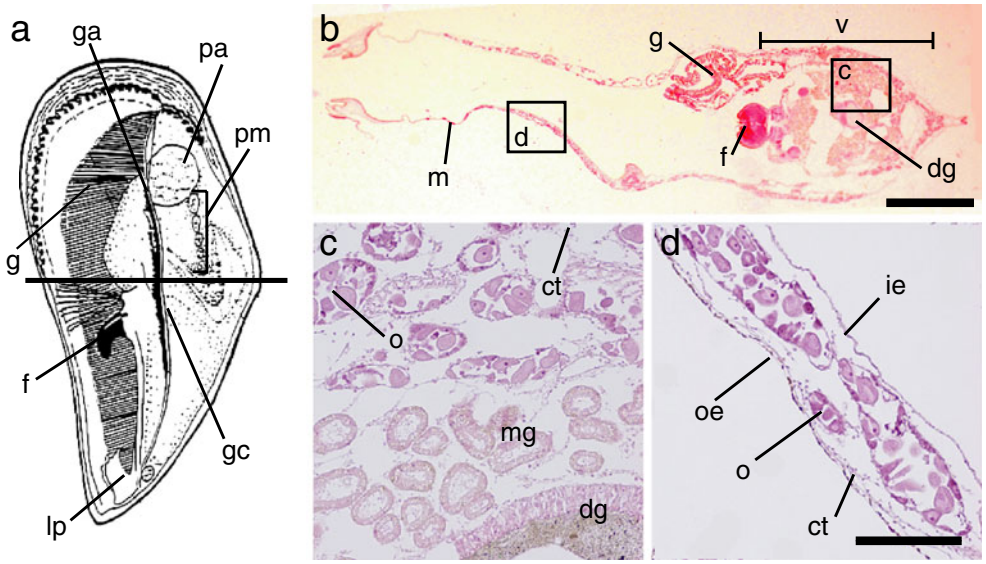

Fig 3 The location of the gonad during the reproductive season. **a** Anatomical schematic diagram of a mature mussel. *Upper side* is posterior. *Right side* is dorsal. A pair of major genital canals is distributed in the dorsal visceral mass along the base of the gill. Genital aperture opens into the mantle cavity between the internal gill and visceral mass. The *black line* shows the plane of **b**. The schematic diagram was modified from the figure taken from the Handbook of Malacology, vol. 1, p. 166. **b**–**d** A section of a female mussel stained with hematoxylin–eosin (HE). **b** cross-section of whole body of a female mussel. The *black squares* show the regions of **c** and **d**. **c** female gonad in the visceral mass. **d** Female gonad in the mantle. *ga* genital aperture, *pa* posterior adductor muscle, *pm* posterior byssal retractor muscle, *g* gill, *f* foot, *gc* genital canal, *lp* labial palp, *m* mantle, *dg* digestive gland, *v* visceral mass, *ct* connective tissue, *mg* midgut gland, *o* ovary, *oe* outer epithelium, *ie* inner epithelium. Scale bar: **b** 500 μm, **d** 200 μm

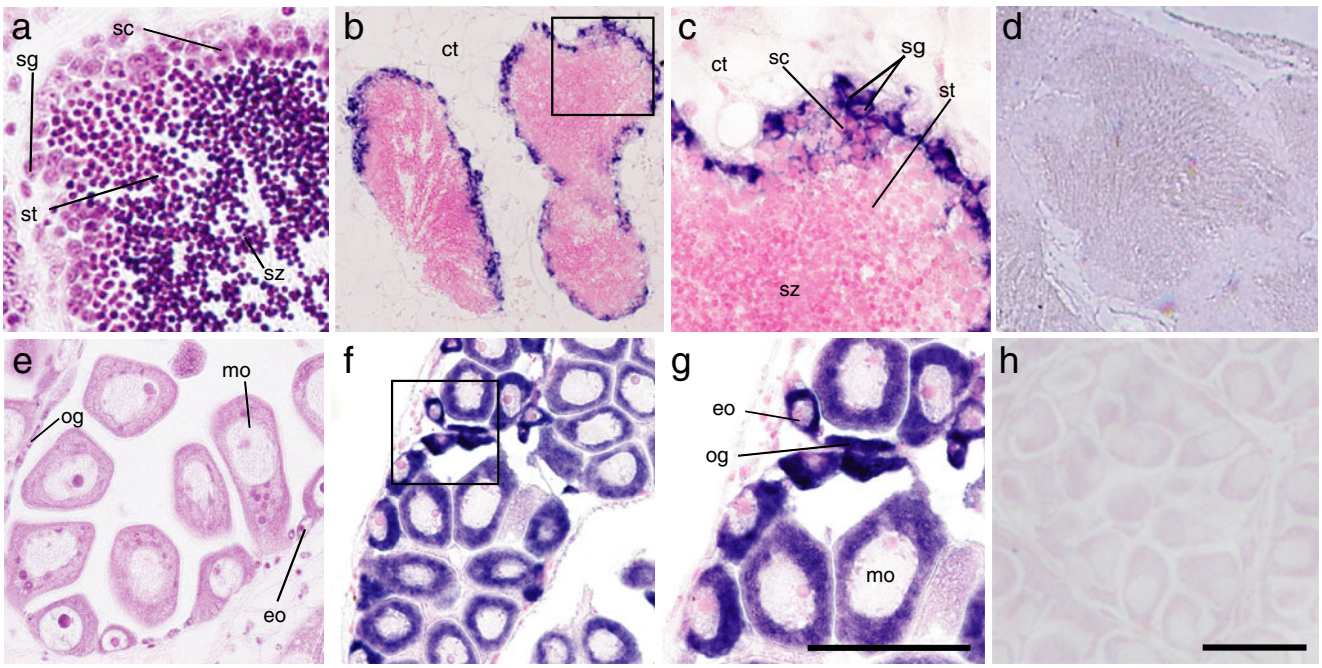

Fig 4 *Myvlg* expression in the mantle in the reproductive season detected with in situ hybridization (ISH). **a**, **e** HE staining, **b**–**d**, **f**–**h** *Myvlg* expression with ISH. Blue signal is *Myvlg* expression. Sections are counterstained by Nuclear Fast Red. **a** Male gonad stained with HE. **b** ISH in a male gonad with antisense probe, **c** high magnification of the *black square* region in **b**. **d** Male gonad with a sense probe. **e** Female gonad stained with HE, **f** ISH in female gonad with an antisense probe. **g** High magnification of the *black square region* in **f**. **h** Female gonad with a sense probe. *sg* spermatogonia, *sc* spermatocyte, *st* spermatid, *sz* spermatozoa, *og* oogonia, *eo* early oocyte, *mo* mature oocyte. Scale bar: 100 μm

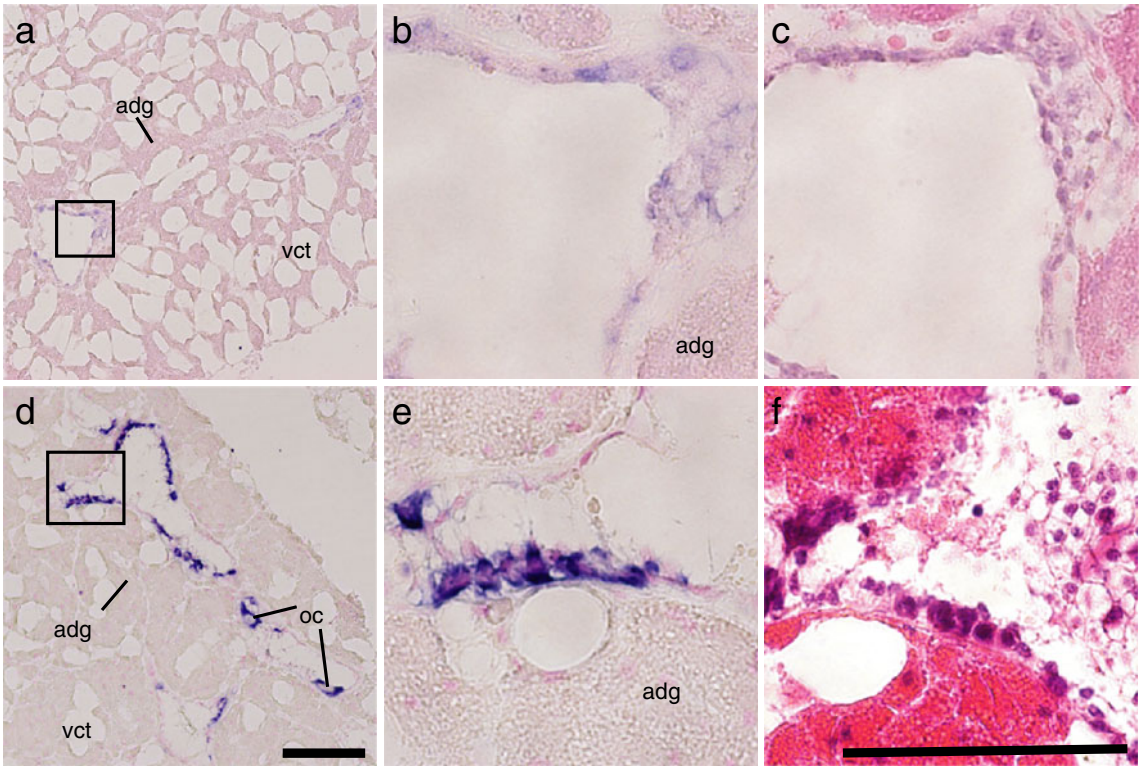

Fig 5 *Myvlg* expression in the connective tissue of the mantle in the non-reproductive season in adult mussels. The sections of ISH staining were counterstained with Nuclear Fast Red. **a**–**c** Mantle at the beginning of the non-reproductive season. **b** High magnification of the *black square region* in **a**. **c** Adjacent section of **b** with HE staining. **d**–**f** Mantle just before the reproductive season. **e** High magnification of *black square* region in **d**. **f** Adjacent section of **e** with HE staining. *adg* adipo-granular tissue, *vct* vesicular connective tissue, *oc* oocyte. Scale bar: 100 μm

brate VASA-like proteins, especially those of the Mollusca. From the *Myvlg* sequence and phylogenetic analysis, the isolated *Myvlg* is considered to be a *vasa* ortholog.

Specific expression of *Myvlg* in the germ line cells

In situ hybridization with *Myvlg*-specific probes revealed that *Myvlg* was specifically expressed in gametes. No expression was detected in somatic tissue. This indicates that *Myvlg* is expressed in germ line cells only, like other *vasa*-related genes (Shibata et al. 1999; Fabioux et al. 2004). *Myvlg*, therefore, is a specific molecular marker for *M. galloprovincialis* germ line cells.

Myvlg expression during the non-reproductive season

In this study, we compared *Myvlg*-positive cells in the non-reproductive season and just before the reproductive season. The number of *Myvlg*-positive cells significantly increased just before the reproductive season, which indicates that *Myvlg*-positive cells proliferated from the non-reproductive to the reproductive season. At just before the reproductive season, we observed oocytes. A feature of GSCs is their pluripotency and ability to self-renew (Lin 1997). From these two results, we suggest that *Myvlg*-positive cells during the non-reproductive season have the feature of GSCs.

GSCs have a big nucleus and little cytoplasm in the non-reproductive season. This characteristic and size is similar to the *Myvlg*-positive cells in immature mussels. *Myvlg*-positive cells in immature mussels may also be GSCs. However, we could not find other morphological characteristics of GSCs because we could not observe ultrastructural features in the cytoplasm with a light microscope. To identify such characteristics of GSCs, further work should be done to detect *Myvlg* expression with a transmission electron microscope.

We stained sections of mussels in the same condition from the non-reproductive and just before the reproductive season. The *Myvlg* signal intensity in the non-reproductive season was much weaker than that from mussels just before and during the reproductive season. This indicates the possibility that the *Myvlg* expression level in GSCs was different between reproductive and non-reproductive mussels. Just before the reproductive season, the number of germ cells increased significantly. We suggest that GSCs do not proliferate during the non-reproductive season when *Myvlg* expression is at a low level. At the beginning of the

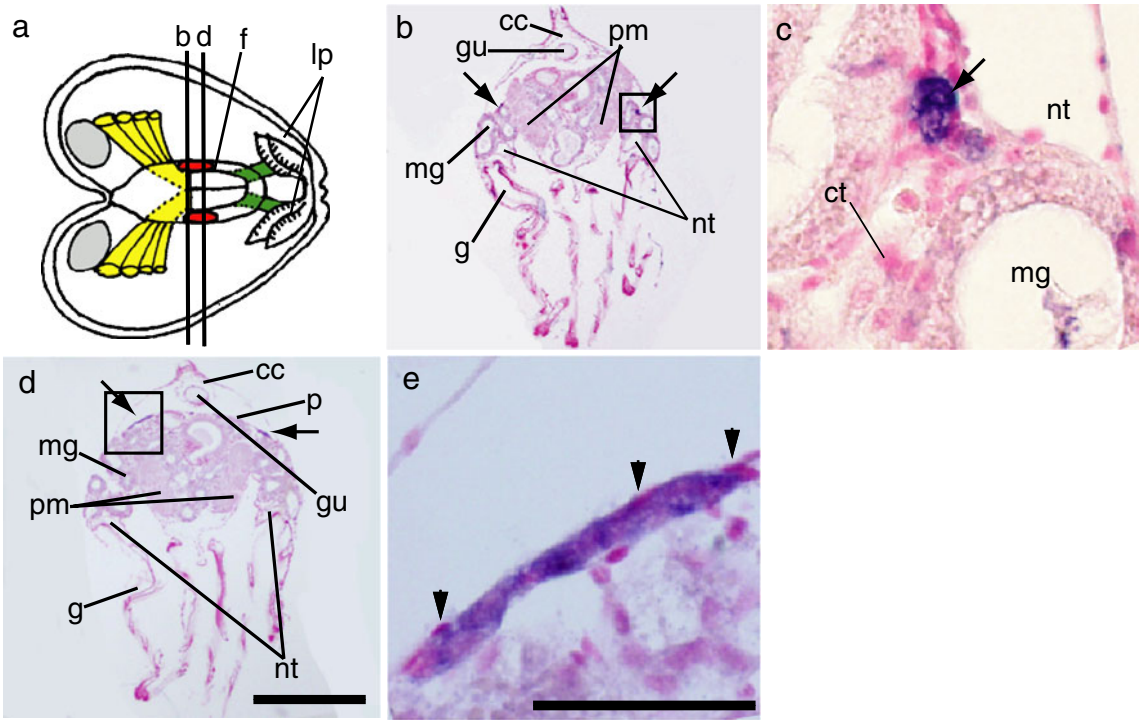

Fig 6 *Myvlg* expression of an immature mussel (shell height, 2–5 mm). The sections were counterstained in Nuclear Fast Red. **a** Explanation of the plane. Diagram shows a mussel opened by cutting the adductor muscle of the shell valves. A pair of gills was removed to expose the mantle. *Left side* is posterior. *Yellow* and *green colored region* indicates posterior and anterior byssal retractor muscles, respectively. *Gray colored region* shows posterior adductor muscle. *Red colored region* shows nephric tubules. The *black line* shows the plane of **b** and **d**, respectively. **b** Section including nephric tubules. **c** High magnification of the *black square region* in **b**. **d** Germ cells along the pericardium. **e** High magnification of the *black square region* in **d**. *f* foot, *lp* labial palps, *nt* nephric tubules, *mg* midgut gland, *pm* posterior byssal retractor muscle, *g* gill, *gu* gut, *cc* cardiac chamber, *ct* connective tissue, *p* pericardium, *arrows* immature germ cells, *arrowheads* flattened somatic cells in the germ cell acinus. Scale bar: **b** 400 μm, **c** 50 μm

reproductive season, GSCs start to proliferate and *Myvlg* expression is high for gametogenesis. However, evidence from real-time PCR is required to demonstrate different *Myvlg* expression levels, since ISH staining is not an accurate tool for quantifying expression levels.

Gonadotropin-releasing hormone (GnRH) and estradiol-17β (E_2) play key roles in the regulation of gametogenesis in many animal species (Pazos and Mathieu 1999). In some bivalve species including oysters, scallops, and *M. galloprovincialis*, GnRH and E_2 induce the proliferation and maturation of germ cells during gametogenesis (Pazos and Mathieu 1999; Janer et al. 2005; Nakamura et al. 2007). Cardinali et al. (2004) reported that E_2 alone, and the combination of E_2 and GnRH induce *vasa* mRNA expression, while GnRH alone significantly decreased *vasa* mRNA expression in the marine teleost, *Sparus aurata*. In bivalves, the expression of *vasa* mRNA may be regulated by hormones like GnRH and E_2 during the reproductive cycle.

Somatic gonadal cells during germ cell migration

Woods (1931) reported that a thin layer of flattened cells surrounds the germ cells in the bivalve *S. striatinum* during gonad formation. In this study, we observed that multiple germ cells formed a cluster attached to flat somatic cell in the acinus. We suggest that germ cells may be supported by specialized somatic cells during migration in the mussel as seen in other animal species. However, we could not observe a fine structure of somatic cells supporting germ cells in this study. The ultrastructure of the somatic gonadal cells should be studied to clarify the function of somatic gonadal tissue.

Distribution of germ cells in immature and mature mussels

The location of PGCs during early development has been reported for one bivalve and one gastropod species (Fabioux et al. 2004; Swartz et al. 2008). Fabioux et al. (2004) found that PGCs were distributed in two symmetrical clumps relative to the midline of embryos, the two clumps corresponding to the Mr and M1 cells derived from the 4d mesentoblast, stem cells of the mesodermal germ bands.

We summarize the process of migration of immature germ cells from metamorphosis to maturation as follows. Immature germ cells are distributed symmetrically and lateral to a pair of nephric tubules in small immature

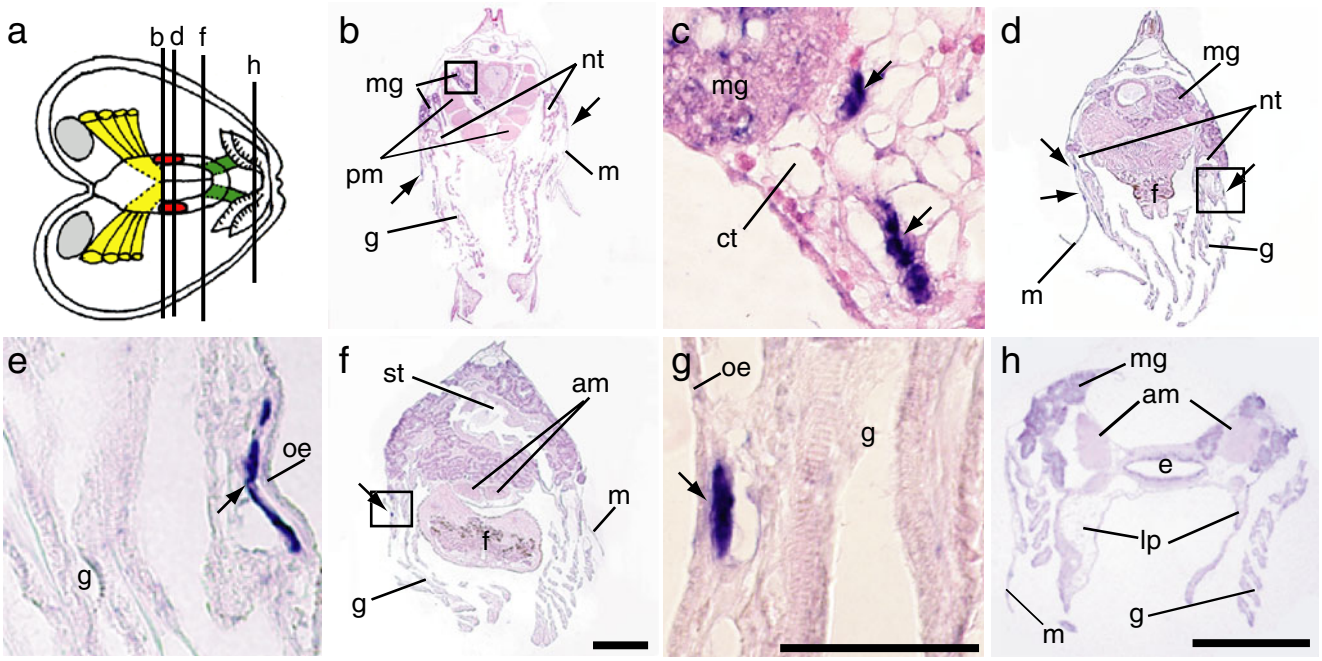

Fig 7 *Myvlg* expression of immature mussels (shell height, 5–15 mm). The sections were counterstained with eosin. **a** Explanation of the plane. The diagram is same as **a**. The *black lines* show the plane of **b**, **d**, **f**, and **h**, respectively. **b** Section including nephric tubules. **c** High magnification of the *black square region* in **d**. Section which was cut through the center of the foot. **e** High magnification of **d**. **f** Section including the anterior byssal retractor muscle. **g** High magnification of **f**. **h** Section including a labial palp and anterior byssal retractor muscle. *mg* midgut gland, *pm* posterior byssal retractor muscle, *nt* nephric tubules, *m* mantle, *g* gill, *f* foot, *ct* connective tissue, *oe* outer epithelium, *st* stomach, *am* anterior byssal retractor muscle, *e* esophagus, *lp* labial palp, *arrows* immature germ cells. Scale bar: **f**, **h** 200 μm, **g** 100 μm

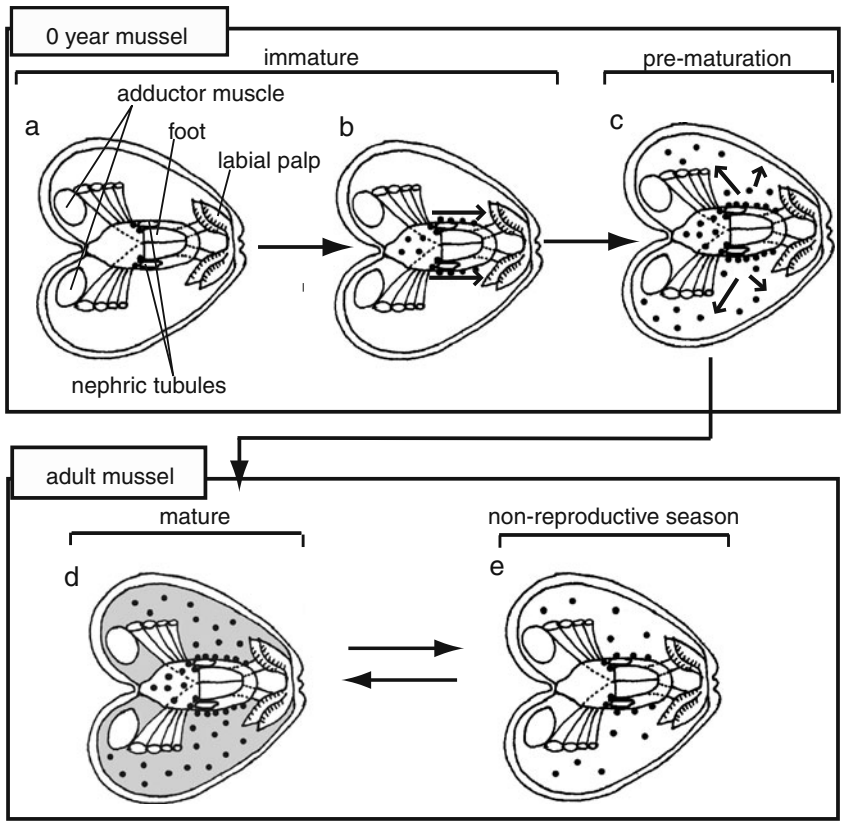

Fig 8 Schematic drawing of germ cell distribution from immature to mature mussels. *Diagram* shows mussel shell opened by cutting the adductor muscle. A pair of gills was removed to expose the mantle. *Black dots* show the distribution of germ cells. *Arrows* show the direction of the migration of the germ cells. *Gray region* shows the location of gametogenesis

mussels (2–5 mm shell height) (Fig. 8a). We suggest that the pair of germ cell clumps observed in this study was also derived from Mr and M1 cells (mesodermal cells). In immature mussels of 5–15 mm shell height, immature germ cells were observed in a region anterior to the nephric tubules. Germ cells formed a pair of lines at the dorsal mantle base between the mantle and gills (Fig. 8b). The number of germ cells in 5–15 mm mussels was significantly greater than that of the 2–5 mm mussels when the number of immature germ cells in the same condition was counted. From these results, we suggest that immature germ cells aggregate in the connective tissue at both lateral sides near the nephric tubules, proliferate, and then migrate anteriorly along the mantle basement. Just before the reproductive season, immature germ cells may become distributed from the dorsal base of the mantle throughout the mantle and visceral mass (Fig. 8c). As a result, gametogenesis occurs in the connective tissue at entire mantle and visceral mass (Fig. 8d). In the non-reproductive season in adult mussels, ADG and VCT developed in the connective tissue of the mantle and visceral mass instead of the gametes. However, GSCs were present in degraded acini of the mantle and visceral mass and *Myvlg* expression was low (Fig. 8e). At the next reproductive season, *Myvlg* expression becomes stronger. GSCs begin to proliferate for gametogenesis to commence.

In this study, therefore, we have shown that immature germ cells proliferate and migrate in immature *M. galloprovincialis*. We have also traced germ line cells during the reproductive cycle by observing the *Myvlg* expression pattern. This is the first report to observe the proliferation and migration of germ cells in immature mussels.

Acknowledgments We thank Misako Miwa for advice on the methodology of in situ hybridization. This study was supported by the Japan Society for the Promotion of Science Research Fellowship for Young Scientists (No. 05488).

References

Cardinali M, Gioacchini G, Candiani S, Pestarino M, Yoshizaki G, Carnevali O (2004) Hormonal regulation of *vasa*-like messenger RNA expression in the ovary of the marine teleost *Sparus aurata*. Biol Reprod 70:737–743

Castrillon DH, Quade BJ, Wang TY, Quigley C, Crum CP (2000) The human VASA gene is specifically expressed in the germ cell lineage. Proc Natl Acad Sci USA 97:9585–9590

Dayhoff MO, Schwartz RM, Orcutt BC (1978) A model of evolutionary change in proteins. In: Atlas of protein sequence and structure. National Biomedical Research Foundation, Silver Spring, MD, pp 345–352

Eddy EM (1975) Germ plasm and the differentiation of the germ cell line. Int Rev Cytol 43:229–281

Fabioux C, Huvet A, Lelong C, Robert R, Pouvreau S, Daniel JY, Minguant C, Le Pennec M (2004) Oyster *vasa*-like gene as a marker of the germ line cell development in *Crassostrea gigas*. Biochem Biophys Res Commun 320:592–598

Fujiwara Y, Komiya T, Kawabata H, Sato M, Fujimoto H, Furusawa M, Noce T (1994) Isolation of a DEAD-family protein gene that encodes a murine homolog of *Drosophila* vasa and its specific expression in germ cell lineage. Proc Natl Acad Sci USA 91:12258–12262

Hay B, Jan LY, Jan YN (1988) A protein component of *Drosophila* polar granules is encoded by *vasa* and has extensive sequence similarity to ATP-dependent helicases. Cell 55:577–587

Heasman J, Quarmby J, Wylie CC (1984) The mitochondrial cloud of *Xenopus* oocytes: the source of germinal granule material. Dev Biol 105:458–469

Janer G, Lavado R, Thibaut R, Porte C (2005) Effects of 17β-estradiol exposure in the mussel *Mytilus galloprovincialis*: a possible regulation role for steroid acyltransferases. Aquat Toxicol 75:32–42

Kautsky N (1982) Quantitative studies on gonad cycle, fecundity, reproductive output and recruitment in a Baltic *Mytilus edulis* population. Mar Biol 68:143–160

Komiya T, Itoh K, Ikenishi K, Furusawa M (1994) Isolation and characterization of a novel gene of the DEAD Box protein family which is specifically expressed in germ cell of *Xenopus laevis*. Dev Biol 162:354–363

Lin H (1997) The tao of stem cells in the germline. Annu Rev Genet 31:455–491

Lowe DM, Moore MN, Bayne BL (1982) Aspects of gametogenesis in the marine mussel *Mytilus edulis* L. J Mar Biol Ass UK 62:133–145

Lubet P (1959) Recherches sur le cycle sexual et l'emission des gametes chez les Mytilides et les Pectinides. Revue Trav Inst (scient tech) Pech marit 23:387–548

Mochizuki K, Nishimiya-Fujisawa C, Fujisawa T (2001) Universal occurrence of the vasa-related genes among metazoans and their germline expression in Hydra. Dev Genes Evol 211:299–308

Nakamura S, Osada M, Kijima A (2007) Involvement of GnRH neuron in the spermatogonial proliferation of the scallop, *Patinopecten yessoensiss*. Mol Reprod Dev 74:108–115

Newell RIE, Hilbish TJ, Koehn RK, Newell CJ (1982) Temporal variation in the reproductive cycle of *Mytilus edulis* L. (Bivalvia Mytilidae) from localities on the east coast of the United States. Biol Bull 162:299–310

Olsen LC, Aasland R, Fjose A (1997) A *vasa*-like gene in zebrafish identifies putative primordial germ cells. Mech Dev 66:95–105

Pazos AJ, Mathieu M (1999) Effects of five natural gonadotropin-releasing hormones on cell suspensions of marine bivalve gonad: stimulation of gonial DNA synthesis. Gen Comp Endocrinol 113:112–120

Pipe RK (1987) Ultrastructural and cytochemical study on interactions between nutrient storage cells and gametogenesis in the mussel *Mytilus edulis*. Mar Biol 96:519–528

Rebscher N, Zelada-Gonzalez F, Banisch TU, Raible F, Arendt D (2007) Vasa unveils a common origin of germ cells and of somatic stem cells from the posterior growth zone in the polychaete *Platynereis dumerilii*. Dev Biol 306:599–611

Roussel D, Bennett KL (1993) glh-1, a germ-line putative RNA helicase from *Caenorhabditis* has four zinc fingers. Proc Natl Acad Sci USA 90:9300–9304

Saffman EE, Lasko P (1999) Germline development in vertebrates and invertebrates. Cell Mol Life Sci 55:1141–1163

Saitou N, Nei M (1987) The neighbor-joining method: a new method for reconstructing phylogenetic trees. Mol Biol Evol 4:406–425

Schmid SR, Linder P (1992) D-E-A-D protein family of putative RNA helicases. Mol Microbiol 6:283–292

Schultz J, Milpetz F, Bork P, Ponting CP (1998) SMART, a simple modular architecture research tool: identification of signaling domains. Proc Natl Acad Sci USA 95:5857–5864

Shibata N, Umesono Y, Orii H, Sakurai T, Watanabe K, Agata K (1999) Expression of vasa (vas)-related genes in germline cells and totipotent somatic stem cells of Planarians. Dev Biol 206:73–87

Swartz SZ, Chan XY, Lambert JD (2008) Localization of *Vasa* mRNA during early cleavage of the snail *Ilyanassa*. Dev Genes Evol 218:107–113

Tamura K, Dudley J, Nei M, Kumar S (2007) MEGA4: molecular evolutionary genetics analysis (MEGA) software version 4.0. Mol Biol Evol 24:1596–1599

Wilkinson DG, Nieto MA (1993) Detection of messenger RNA by in situ hybridization to tissue sections and whole-mounts. Methods Enzymol 225:361–373

Woods FH (1931) History of the germ cells in Sphaerium striatinum (Lam.). J Morphol 51:545–595

Woods FH (1932) Keimbahn determinants and continuity of the germ cells in *Sphaerium striatinum* (Lam.). J Morphol 53:345–365

Yoshizaki G, Sakatani S, Tominaga H, Takeuchi T (2000) Cloning and characterization of a vasa-like gene in rainbow trout and its expression in the germ cell lineage. Mol Reprod Dev 55:364–371